Available online at www.sciencedirect.com

ScienceDirect

Journal of Computational and Applied Mathematics 200 (2007) 705 – 721

JOURNAL OF COMPUTATIONAL AND APPLIED MATHEMATICS

www.elsevier.com/locate/cam

Uniform convergence of a weighted average scheme for a nonlinear reaction–diffusion problem

Igor Boglaev[a,*], Matthew Hardy[b]

[a] Institute of Fundamental Sciences, Massey University, Private Bag 11-222, Palmerston North, New Zealand
[b] Mathematical Sciences Institute, Australian National University, Canberra 0200, Australia

Received 22 July 2005

Abstract

This paper deals with a weighted average scheme (or θ-scheme) for solving a nonlinear singularly perturbed parabolic reaction–diffusion problem. The uniform convergence of the weighted average scheme on piecewise uniform and log-meshes is established. Numerical experiments are presented.

Keywords: Parabolic reaction–diffusion problem; Boundary layers; Weighted average scheme; Uniform convergence

1. Introduction

We are interested in solving the nonlinear reaction–diffusion problem

$$-\mu^2(u_{xx}+u_{yy})+u_t=-f(x,y,t,u), \tag{1}$$

$$(x,y,t)\in Q=\omega\times(0,t_F], \quad \omega=\{0<x<1,0<y<1\},$$

$$0\leqslant f_u\leqslant c_*=\text{const} \quad (x,y,t,u)\in\overline{Q}\times(-\infty,\infty) \;\; (f_u\equiv\partial f/\partial u),$$

where μ is a small positive parameter. The initial-boundary conditions are defined by

$$u(x,y,0)=u^0(x,y), \quad (x,y)\in\overline{\omega},$$

$$u(x,y,t)=g(x,y,t), \quad (x,y,t)\in\partial\omega\times(0,t_F],$$

where $\partial\omega$ is the boundary of ω. The functions f, g and u^0 are sufficiently smooth. Under suitable continuity and compatibility conditions on the data, a unique solution u of (1) exists (see [6] for details). For $\mu\ll 1$, problem (1) is singularly perturbed and characterized by the boundary layers of width $O(\mu|\ln\mu|)$ at the boundary $\partial\omega$ (see Section 3.2 for details). We mention that the assumption $f_u\geqslant 0$ in (1) can always be obtained via a change of variables.

* Corresponding author.
E-mail addresses: I.Boglaev@massey.ac.nz (I. Boglaev), matthew.hardy@anu.edu.au (M. Hardy).

0377-0427/$ - see front matter
doi:10.1016/j.cam.2006.01.026

It is well-known that classical numerical methods for solving singularly perturbed problems are inefficient, since in order to resolve layers they require a fine mesh covering the whole domain. For constructing efficient numerical algorithms to handle these problems, there are two general approaches: the first one is based on layer-adapted meshes and the second is based on exponential fitting or on locally exact schemes. The basic property of the efficient numerical methods is uniform convergence with respect to the perturbation parameter. The three books [4,7,9] develop these approaches and give comprehensive applications to wide classes of singularly perturbed problems.

Our goal is to construct a μ-uniform numerical method for solving problem (1), that is, a numerical method which generates μ-uniformly convergent numerical approximations to the solution. We use a numerical method based on a weighted average scheme. This 10-point difference scheme can be regarded as taking a weighted average of the explicit scheme and the implicit scheme.

We mention that in [5], the uniform convergence of the weighted average scheme on the piecewise uniform mesh of Shishkin-type [12], applied to a linear one-dimensional parabolic problem, was proved.

The structure of the paper is as follows. In Section 2, we construct the nonlinear difference scheme based on the weighted average scheme. Section 3 deals with the uniform convergence of the weighted average scheme on the piecewise uniform and log-meshes. The numerical experiments of Section 4 use the monotone iterative method to solve the weighted average scheme. The accuracy is investigated for two types of layer-adapted meshes. The numerical evidence further clarifies the theoretical stability constraints and convergence order estimates.

2. The weighted average scheme

On $\overline{Q}$ introduce a rectangular mesh $\overline{\omega}^h \times \overline{\omega}^\tau$, $\overline{\omega}^h = \overline{\omega}^{hx} \times \overline{\omega}^{hy}$:

$$\overline{\omega}^{hx} = \{x_i,\ 0 \leqslant i \leqslant N_x;\ x_0 = 0,\ x_{N_x} = 1;\ h_{xi} = x_{i+1} - x_i\},$$

$$\overline{\omega}^{hy} = \{y_j,\ 0 \leqslant j \leqslant N_y;\ y_0 = 0,\ y_{N_y} = 1;\ h_{yj} = y_{j+1} - y_j\},$$

$$\overline{\omega}^{\tau} = \{t_k = k\tau,\ 0 \leqslant k \leqslant N_\tau,\ N_\tau \tau = t_F\}.$$

For a mesh function $U(P,t)$, $P = (x,y) \in \overline{\omega}^h$, $t \in \overline{\omega}^\tau$, we use the weighted average or θ-scheme

$$\theta \mathscr{L}^h U(P,t) + (1-\theta)\mathscr{L}^h U(P,t-\tau) + \frac{1}{\tau}[U(P,t) - U(P,t-\tau)] = -\mathscr{F}^\tau, \tag{2}$$

$$\mathscr{F}^\tau \equiv \theta f(P,t,U) + (1-\theta) f(P,t-\tau,U), \quad (P,t) \in \omega^h \times \omega^\tau,$$

$$U(P,t) = g(P,t),\ (P,t) \in \partial\omega^h \times \omega^\tau, \quad U(P,0) = u^0(P), \quad P \in \overline{\omega}^h,$$

where $\theta = \text{const}$ and, when no confusion arises, we write $f(P,t,U(P,t)) = f(P,t,U)$. The linear operator $\mathscr{L}^h$ is defined by

$$\mathscr{L}^h U = -\mu^2(\mathscr{D}_x^2 U + \mathscr{D}_y^2 U),$$

where $\mathscr{D}_x^2 U$ and $\mathscr{D}_y^2 U$ are the central difference approximations to the second derivatives

$$\mathscr{D}_x^2 U_{ij}^k = (\hbar_{xi})^{-1}[(U_{i+1,j}^k - U_{ij}^k)(h_{xi})^{-1} - (U_{ij}^k - U_{i-1,j}^k)(h_{x,i-1})^{-1}],$$

$$\mathscr{D}_y^2 U_{ij}^k = (\hbar_{yj})^{-1}[(U_{i,j+1}^k - U_{ij}^k)(h_{yj})^{-1} - (U_{ij}^k - U_{i,j-1}^k)(h_{y,j-1})^{-1}],$$

$$\hbar_{xi} = 2^{-1}(h_{x,i-1} + h_{xi}), \quad \hbar_{yj} = 2^{-1}(h_{y,j-1} + h_{yj}),$$

where $U_{ij}^k \equiv U\left(x_i, y_j, t_k\right)$.

This 10-point difference scheme can be regarded as taking a weighted average of the explicit scheme ($\theta = 0$) and the implicit scheme ($\theta = 1$). We shall assume that we are using an average with nonnegative weights, so that $0 \leqslant \theta \leqslant 1$.

3. Uniform convergence of the difference scheme (2)

Here we analyze uniform convergence properties of the θ-method (2). Introduce the following notation:

$$
\begin{aligned}
&v_i = v_{x,i-1} + v_{xi}, \quad v_{x,i-1} = (\hbar_{xi})^{-1}(h_{x,i-1})^{-1}, \quad v_{xi} = (\hbar_{xi})^{-1}(h_{xi})^{-1}, \\
&w_j = w_{y,j-1} + w_{yj}, \quad w_{y,j-1} = (\hbar_{yj})^{-1}(h_{y,j-1})^{-1}, \quad w_{yj} = (\hbar_{yj})^{-1}(h_{yj})^{-1}, \\
&\bar{v} = \max_{1 \leqslant i \leqslant N_x - 1} v_i, \quad \bar{w} = \max_{1 \leqslant j \leqslant N_y - 1} w_j.
\end{aligned}
\tag{3}
$$

Suppose that the time mesh spacing τ satisfies the constraint

$$
\tau(1-\theta) \leqslant \frac{1}{\mu^2(\bar{v} + \bar{w}) + c^*}. \tag{4}
$$

The condition (4) guarantees the discrete maximum principle on the computational domain $\overline{\omega}^h \times \overline{\omega}^\tau$. For the implicit difference scheme with $\theta = 1$, there is no restriction on the time spacing τ.

The constraint of type (4) is known as the CFL condition. For the θ-method on the uniform mesh with step sizes h_x and h_y in the x- and y-directions, respectively, the condition (4) can be represented in the standard form

$$
(v_x + v_y)(1-\theta) \leqslant 0.5, \quad v_x = \frac{\mu^2 \tau}{h_x^2}, \quad v_y = \frac{\mu^2 \tau}{h_y^2}.
$$

In the case of the linear one-dimensional differential equation $-\mu^2 u_{xx} + u_t = -f(x,t)$, we obtain the condition $v(1-\theta) \leqslant 0.5$ from [8].

The case $\theta = 0.5$ corresponds to the Crank–Nicolson difference scheme [3]. It is well-known that for a linear problem (1) with constant coefficients, the Fourier analysis leads to the unconditionally stable Crank–Nicolson difference scheme. We know mathematically (and by common experience if u represents, say, temperature) that $u(x, y, t)$ is bounded above and below by the extremes attained by the initial data and the values on the boundary up to time t.

In the case of the linear one-dimensional differential equation $-\mu^2 u_{xx} + u_t = 0$, the condition (4), $v(1-\theta) \leqslant 0.5$, is very much more restrictive than that needed in the Fourier analysis of stability, $v(1-2\theta) \leqslant 0.5$. For example, the Crank–Nicolson scheme always satisfies the stability condition, but only if $v \leqslant 1$ does it satisfy the condition given for the maximum principle. In view of this large gap one may wonder about the sharpness of this condition. In fact, the maximum principle condition is sharp, but a little severe; with $N_x = 2$, $U_0^0 = U_2^0 = 0$, $U_1^0 = 1$ and $g(0,t) = g(1,t) = 0$, it follows that $U_1^1 = (1 - 2(1-\theta)v)/(1 + 2\theta v)$ which is nonnegative only if the given condition is satisfied.

Thus, the maximum principle analysis can be viewed as an alternative means of obtaining stability conditions. It has the advantage over Fourier analysis that it is easily extended to problems with variable coefficients and to nonlinear problems as well. We mention here that, in general, the maximum principle analysis gives only sufficient conditions for stability of difference schemes.

3.1. Truncation error of the difference scheme (2)

Firstly, we consider the Crank–Nicolson difference (2) with $\theta = 0.5$. Fix $t \in \omega^\tau$ and $(x_i, y_j) \in \omega^h$, and introduce the one-dimensional differential equation in the space variable x,

$$
\begin{aligned}
&\mu^2 \frac{d^2 u(x, y_j, t)}{dx^2} = \psi^{(x)}(x, y_j, t), \quad x_i < x < x_{i+1}, \\
&\psi^{(x)}(x, y_j, t) \equiv \frac{1}{2} f(x, y_j, t, u(x, y_j, t)) + \frac{1}{2} \frac{\partial u(x, y_j, t)}{\partial t}.
\end{aligned}
$$

Using the Green function $G_i^{(x)}$ of the differential operator $\mu^2 \mathrm{d}^2/\mathrm{d}x^2$ on $[x_i, x_{i+1}]$, we represent the exact solution $u(x, y_j, t)$ in the form

$$u(x, y_j, t) = u(x_i, y_j, t)\phi_{1i}(x) + u(x_{i+1}, y_j, t)\phi_{2i}(x) + \int_{x_i}^{x_{i+1}} G_i^{(x)}(x, s)\psi^{(x)}(s, y_j, t)\,\mathrm{d}s,$$

where the local Green function $G_i^{(x)}$ is given by

$$G_i^{(x)}(x, s) = \frac{1}{\mu^2 w_i^{(x)}(s)} \begin{cases} \phi_{1i}(s)\phi_{2i}(x), & x \leqslant s, \\ \phi_{1i}(x)\phi_{2i}(s), & x \geqslant s, \end{cases}$$

$$w_i^{(x)}(s) = \phi_{2i}(s)[\phi_{1i}(x)]'_{x=s} - \phi_{1i}(s)[\phi_{2i}(x)]'_{x=s},$$

and $\phi_{1i}(x),\ \phi_{2i}(x)$ are defined by

$$\phi_{1i}(x) = \frac{x_{i+1} - x}{h_{xi}}, \quad \phi_{2i}(x) = \frac{x - x_i}{h_{xi}}, \quad x_i \leqslant x \leqslant x_{i+1}.$$

Equating the derivatives $\mathrm{d}u(x_i - 0, y_j, t)/\mathrm{d}x$ and $\mathrm{d}u(x_i + 0, y_j, t)/\mathrm{d}x$, we get the following integral-difference formula

$$\mu^2 \mathscr{D}_x^2 u(x_i, y_j, t) = \frac{1}{\hbar_{xi}} \int_{x_{i-1}}^{x_i} \phi_{2,i-1}(s)\psi^{(x)}(s, y_j, t)\,\mathrm{d}s + \frac{1}{\hbar_{xi}} \int_{x_i}^{x_{i+1}} \phi_{1i}(s)\psi^{(x)}(s, y_j, t)\,\mathrm{d}s. \tag{5}$$

Now, representing $\psi^{(x)}(x, y_j, t)$ on $[x_{i-1}, x_{i+1}]$ in the form

$$\psi^{(x)}(x, y_j, t) = \psi(x_i, y_j, t) + \int_{x_i}^{x} \frac{\mathrm{d}\psi^{(x)}}{\mathrm{d}s}\,\mathrm{d}s,$$

the above integral-difference formula can be written as

$$\mu^2 \mathscr{D}_x^2 u(P, t) = \frac{1}{2} f(P, t, u) + \frac{1}{2}\frac{\partial u(P, t)}{\partial t} + I^{(x)}(P, t, u), \quad (P, t) \in \omega^h \times \omega^\tau,$$

where we denote

$$\begin{aligned} I^{(x)}(x_i, y_j, t, u) \equiv{}& \frac{1}{\hbar_{xi}} \int_{x_{i-1}}^{x_i} \phi_{2,i-1}(s) \left(\int_{x_i}^{s} \frac{\mathrm{d}\psi^{(x)}(\xi, y_j, t)}{\mathrm{d}\xi}\,\mathrm{d}\xi \right) \mathrm{d}s \\ &+ \frac{1}{\hbar_{xi}} \int_{x_i}^{x_{i+1}} \phi_{1i}(s) \left(\int_{x_i}^{s} \frac{\mathrm{d}\psi^{(x)}(\xi, y_j, t)}{\mathrm{d}\xi}\,\mathrm{d}\xi \right) \mathrm{d}s. \end{aligned} \tag{6}$$

Similarly, for the one-dimensional differential equation in the space variable y

$$\mu^2 \frac{\mathrm{d}^2 u(x_i, y, t)}{\mathrm{d}y^2} = \psi^{(y)}(x_i, y, t), \quad y_j < y < y_{j+1},$$

$$\psi^{(y)}(x_i, y, t) \equiv \frac{1}{2} f(x_i, y, t, u(x_i, y, t)) + \frac{1}{2}\frac{\partial u(x_i, y, t)}{\partial t},$$

we can prove the formula

$$\mu^2 \mathscr{D}_y^2 u(P, t) = \frac{1}{2} f(P, t, u) + \frac{1}{2}\frac{\partial u(P, t)}{\partial t} + I^{(y)}(P, t, u), \quad (P, t) \in \omega^h \times \omega^\tau,$$

where we denote

$$I^{(y)}(x_i, y_j, t, u) \equiv \frac{1}{\hbar_{yi}} \int_{y_{j-1}}^{y_j} \varphi_{2,j-1}(s) \left(\int_{y_j}^{s} \frac{\mathrm{d}\psi^{(y)}(x_i, \xi, t)}{\mathrm{d}\xi} \, \mathrm{d}\xi \right) \mathrm{d}s + \frac{1}{\hbar_{yi}} \int_{y_j}^{y_{j+1}} \varphi_{1j}(s) \left(\int_{y_j}^{s} \frac{\mathrm{d}\psi^{(y)}(x_i, \xi, t)}{\mathrm{d}\xi} \, \mathrm{d}\xi \right) \mathrm{d}s, \tag{7}$$

where $\varphi_{1j}(y)$ and $\varphi_{2j}(y)$ are defined by

$$\varphi_{1j}(y) = \frac{y_{j+1} - y}{h_{yj}}, \quad \varphi_{2j}(y) = \frac{y - y_j}{h_{yj}}, \quad y_j \leqslant y \leqslant y_{j+1}.$$

Thus, the exact solution u to (1) satisfies the integral-difference equation

$$\mathscr{L}^h u(P, t) + \frac{\partial u(P, t)}{\partial t} = -f(P, t, u) - I(P, t, u), \quad (P, t) \in \omega^h \times \omega^\tau,$$

$$I(P, t, u) \equiv [I^{(x)}(P, t, u) + I^{(y)}(P, t, u)],$$

where the difference operator $\mathscr{L}^h$ is defined in (2). From here and (2), it follows that for $\theta = 0.5$, the truncation error $T(P, t)$ can be represented in the form

$$T(P, t) = T_1(P, t) - \tfrac{1}{2}[I(P, t, u) + I(P, t - \tau, u)],$$

$$T_1(P, t) \equiv \frac{u(P, t) - u(P, t - \tau)}{\tau} - \frac{1}{2}\left[\frac{\partial u(P, t)}{\partial t} + \frac{\partial u(P, t - \tau)}{\partial t}\right].$$

Using the Taylor expansions about the center of the 10 mesh points, namely $(P, t_{1/2})$, $t_{1/2} \equiv t - \frac{1}{2}\tau$, we obtain

$$T_1(P, t) = \tfrac{1}{48}\tau^2 u_{ttt}(P, t^a_{1/2}) + \tfrac{1}{48}\tau^2 u_{ttt}(P, t^b_{1/2}) - \tfrac{1}{16}\tau^2 u_{ttt}(P, t^c_{1/2}) - \tfrac{1}{16}\tau^2 u_{ttt}(P, t^d_{1/2}),$$

$$t_{1/2} < t^{a,c}_{1/2} < t, \quad t - \tau < t^{b,d}_{1/2} < t_{1/2}.$$

Thus, we have proved the following lemma.

Lemma 1. *The truncation error of the Crank–Nicolson scheme* (2), $\theta = 0.5$, *can be estimated by*

$$\|T(t)\|_{\omega^h} \leqslant \tfrac{1}{6} \max_{(x,y,t)\in Q} |u_{ttt}(x, y, t)|\tau^2 + \tfrac{1}{2}[\|I(t)\|_{\omega^h} + \|I(t - \tau)\|_{\omega^h}], \tag{8}$$

where $I(P, t, u) = I^{(x)}(P, t, u) + I^{(y)}(P, t, u)$, $I^{(x)}(P, t, u)$ *and* $I^{(y)}(P, t, u)$ *are defined in* (6) *and* (7), *respectively*.

For $\theta \in [0, 1]\backslash\{0.5\}$, the truncation error $T(P, t)$ can be represented in the form

$$T(P, t) = T_1(P, t) - [\theta I(P, t, u) + (1 - \theta)I(P, t - \tau, u)],$$

$$T_1(P, t) \equiv \frac{u(P, t) - u(P, t - \tau)}{\tau} - \left[\theta\frac{\partial u(P, t)}{\partial t} + (1 - \theta)\frac{\partial u(P, t - \tau)}{\partial t}\right].$$

Using the Taylor expansions about a mesh point (P, t), we obtain

$$T_1(P, t) = -\tfrac{1}{2}\tau u_{tt}(P, t^a_\theta) + (1 - \theta)\tau u_{tt}(P, t^b_\theta), \quad t - \tau < t^{a,b}_\theta < t.$$

Thus, we prove the following lemma.

Lemma 2. *The truncation error of the difference scheme* (2) *for* $\theta \in [0, 1]\backslash\{0.5\}$ *can be estimated in the form*

$$\|T(t)\|_{\omega^h} \leqslant \left(\frac{3}{2} - \theta\right) \max_{(x,y,t)\in Q} |u_{tt}(x, y, t)|\tau + \theta\|I(t)\|_{\omega^h} + (1-\theta)\|I(t-\tau)\|_{\omega^h}. \tag{9}$$

3.2. Bounds on $I^{(x)}$ and $I^{(y)}$ from (6), (7)

We suppose sufficient smoothness of functions f, g and u^0 in (1) and also sufficient compatibility conditions between the initial and boundary data, in such a way that for l sufficiently large integer and $0 < \alpha < 1$, the solution of (1) satisfies

$$u(x, y, t) \in C^{l+\alpha, l+\alpha, (l+\alpha)/2}(\overline{\omega} \times [0, t_F]).$$

Using the mean-value theorem, the right-hand side in (1) can be written in the form $f(x, y, t, u) = f(x, y, t, 0) + f_u u$. Now, we may consider (1) as a linear equation with the smooth coefficient f_u and use the bounds of the exact solution and its derivatives obtained in [12] for a linear problem. According to [12], the solution can be decomposed into two parts $u = S + E$, where S and E are the regular and singular parts of u, respectively. In turn, the singular part can be decomposed in the form

$$E = \Phi + \Psi + (\Upsilon_{00} + \Upsilon_{10} + \Upsilon_{01} + \Upsilon_{11}),$$

where Φ and Ψ are essentially one-dimensional boundary layer functions in some neighborhoods of sides $x = 0$, $x = 1$ and $y = 0$, $y = 1$, respectively, and Υ_{mn}, $m, n = 0, 1$ are corner layers in the neighborhood of (m, n). According to the results from [12], the following bounds hold true:

$$\left|\frac{\partial^k S(x, y, t)}{\partial x^{k_x} \partial y^{k_y} \partial t^{k_t}}\right| \leqslant C, \tag{10}$$

$$\left|\frac{\partial^k \Phi(x, y, t)}{\partial x^{k_x} \partial y^{k_y} \partial t^{k_t}}\right| \leqslant C\mu^{-k_x}\Pi(x), \quad \Pi(x) = \Pi_0(x) + \Pi_1(x),$$

$$\left|\frac{\partial^k \Psi(x, y, t)}{\partial x^{k_x} \partial y^{k_y} \partial t^{k_t}}\right| \leqslant C\mu^{-k_y}\hat{\Pi}(y), \quad \hat{\Pi}(y) = \hat{\Pi}_0(y) + \hat{\Pi}_1(y),$$

$$\left|\frac{\partial^k \Upsilon_{mn}(x, y, t)}{\partial x^{k_x} \partial y^{k_y} \partial t^{k_t}}\right| \leqslant C\mu^{-(k_y+k_y)}\Pi_m(x)\hat{\Pi}_n(y), \quad m, n = 0, 1,$$

$$\Pi_0(x) = \exp(-\kappa_1 x/\mu), \quad \Pi_1(x) = \exp(-\kappa_1(1-x)/\mu),$$

$$\hat{\Pi}_0(y) = \exp(-\kappa_2 y/\mu), \quad \hat{\Pi}_1(y) = \exp(-\kappa_2(1-y)/\mu),$$

where $k = (k_x, k_y, k_t)$, $k_x + k_y + 2k_t \leqslant l$, and here and throughout C denotes a generic positive constant which is independent of μ and the mesh parameters.

From (6), it follows that

$$|I^{(x)}(x_i, y_j, t, u)| \leqslant \frac{1}{\hbar_{xi}} \int_{x_{i-1}}^{x_i} \phi_{2,i-1}(s) \left(\int_{x_{i-1}}^{x_i} \left|\frac{d\psi^{(x)}(\xi, y_j, t)}{d\xi}\right| d\xi\right) ds + \frac{1}{\hbar_{xi}} \int_{x_i}^{x_{i+1}} \phi_{1i}(s) \left(\int_{x_i}^{x_{i+1}} \left|\frac{d\psi^{(x)}(\xi, y_j, t)}{d\xi}\right| d\xi\right) ds.$$

From (10), the following estimate on $d\psi^{(x)}/dx$ holds true

$$\left|\frac{d\psi^{(x)}(x, y_j, t)}{dx}\right| \leqslant C[1 + \mu^{-1}\Pi(x)], \quad 0 \leqslant x \leqslant 1,$$

and on the intervals $[0, \frac{1}{2}]$ and $[\frac{1}{2}, 1]$, we have

$$\left|\frac{\mathrm{d}\psi^{(x)}(x, y_j, t)}{\mathrm{d}x}\right| \leqslant C[1 + \mu^{-1}\Pi_0(x)], \quad 0 \leqslant x \leqslant \tfrac{1}{2},$$

$$\left|\frac{\mathrm{d}\psi^{(x)}(x, y_j, t)}{\mathrm{d}x}\right| \leqslant C[1 + \mu^{-1}\Pi_1(x)], \quad \tfrac{1}{2} \leqslant x \leqslant 1.$$

Hence, we obtain

$$|I^{(x)}(x_i, y_j, t, u)| \leqslant \frac{C}{2\hbar_{xi}}[(h_{xi-1}^2 + h_{xi}^2) + B_1(h_{xi-1}, x_{i-1}) + B_1(h_{xi}, x_i)],$$

$$x_i \in (0, \tfrac{1}{2}], \quad B_1(v, w) \equiv \frac{v}{\kappa_1}\exp(-\mu^{-1}\kappa_1 w)[1 - \exp(-\mu^{-1}\kappa_1 v)],$$

$$|I^{(x)}(x_i, y_j, t, u)| \leqslant \frac{C}{2\hbar_{xi}}[(h_{xi-1}^2 + h_{xi}^2) + B_1(h_{xi-1}, 1 - x_i) + B_1(h_{xi}, 1 - x_{i+1})], \quad x_i \in [\tfrac{1}{2}, 1). \tag{11}$$

Similarly, $I^{(y)}(x_i, y_j, t, u)$ is estimated by

$$|I^{(y)}(x_i, y_j, t, u)| \leqslant \frac{C}{2\hbar_{yj}}[(h_{yj-1}^2 + h_{yj}^2) + B_2(h_{yj-1}, y_{j-1}) + B_2(h_{yj}, y_j)],$$

$$y_j \in (0, \tfrac{1}{2}], \quad B_2(v, w) \equiv \frac{v}{\kappa_2}\exp(-\mu^{-1}\kappa_2 w)[1 - \exp(-\mu^{-1}\kappa_2 v)],$$

$$|I^{(y)}(x_i, y_j, t, u)| \leqslant \frac{C}{2\hbar_{yj}}[(h_{yj-1}^2 + h_{yj}^2) + B_2(h_{yj-1}, 1 - y_j) + B_2(h_{yj}, 1 - y_{j+1})], \quad y_j \in [\tfrac{1}{2}, 1). \tag{12}$$

3.3. The difference scheme (2) on special fitted meshes

Here we estimate convergence properties of the difference (2) defined on meshes of general type introduced in [10].

A mesh of this type is formed in the following manner. We divide each of the intervals $\overline{\omega}^x = [0, 1]$ and $\overline{\omega}^y = [0, 1]$ into three parts $[0, \sigma_x]$, $[\sigma_x, 1 - \sigma_x]$, $[1 - \sigma_x, 1]$, and $[0, \sigma_y]$, $[\sigma_y, 1 - \sigma_y]$, $[1 - \sigma_y, 1]$, respectively. Assuming that N_x, N_y are divisible by 4, in the parts $[0, \sigma_x]$, $[1 - \sigma_x, 1]$ and $[0, \sigma_y]$, $[1 - \sigma_y, 1]$ we allocate $N_x/4 + 1$ and $N_y/4 + 1$ mesh points, respectively, and in the parts $[\sigma_x, 1 - \sigma_x]$ and $[\sigma_y, 1 - \sigma_y]$ we allocate $N_x/2 + 1$ and $N_y/2 + 1$ mesh points, respectively. Points σ_x, $(1 - \sigma_x)$ and σ_y, $(1 - \sigma_y)$ correspond to transition to the boundary layers. We consider meshes $\overline{\omega}^{hx}$ and $\overline{\omega}^{hy}$ which are equidistant in $[x_{N_x/4}, x_{3N_x/4}]$ and $[y_{N_y/4}, y_{3N_y/4}]$ but graded in $[0, x_{N_x/4}]$, $[x_{3N_x/4}, 1]$ and $[0, y_{N_y/4}]$, $[y_{3N_y/4}, 1]$. On $[0, x_{N_x/4}]$, $[x_{3N_x/4}, 1]$ and $[0, y_{N_y/4}]$, $[y_{3N_y/4}, 1]$ let our mesh be given by a mesh generating function d with $d(0) = 0$ and $d(1/4) = 1$ which is supposed to be continuous, monotonically increasing, and piecewise continuously differentiable. Then our mesh is defined by

$$x_i = \begin{cases} \sigma_x d(\xi_i), & \xi_i = i/N_x, \quad i = 0, \ldots, N_x/4, \\ \sigma_x + (i - N_x/4)h_x, & i = N_x/4 + 1, \ldots, 3N_x/4, \\ 1 - \sigma_x d(\xi_i), & \xi_i = (N_x - i)/N_x, \quad i = 3N_x/4 + 1, \ldots, N_x, \end{cases}$$

$$y_j = \begin{cases} \sigma_y d(\xi_j), & \xi_j = j/N_y, \quad j = 0, \ldots, N_y/4, \\ \sigma_y + (j - N_y/4)h_y, & j = N_y/4 + 1, \ldots, 3N_y/4, \\ 1 - \sigma_y d(\xi_j), & \xi_j = (N_y - j)/N_y, \quad j = 3N_y/4 + 1, \ldots, N_y, \end{cases}$$

$$h_x = 2(1 - 2\sigma_x)N_x^{-1}, \quad h_y = 2(1 - 2\sigma_y)N_y^{-1}.$$

We also assume that $d(d(\xi))/d\xi$ does not decrease. This condition implies that

$$h_{xi} \leqslant h_{x,i+1}, \quad i = 1, \ldots, N_x/4 - 1, \quad h_{xi} \geqslant h_{x,i+1}, \quad i = 3N_x/4 + 1, \ldots, N_x - 1,$$
$$h_{yj} \leqslant h_{y,j+1}, \quad j = 1, \ldots, N_y/4 - 1, \quad h_{yj} \geqslant h_{y,j+1}, \quad j = 3N_y/4 + 1, \ldots, N_y - 1.$$

3.3.1. Uniform convergence of the difference scheme (2) on the piecewise uniform mesh

We choose the transition points σ_x, $(1 - \sigma_x)$ and σ_y, $(1 - \sigma_y)$ as in [12], i.e.,

$$\sigma_x = \min\{4^{-1}, \upsilon_1 \mu \ln N_x\}, \quad \sigma_y = \min\{4^{-1}, \upsilon_2 \mu \ln N_y\},$$

where υ_1 and υ_2 are positive constants. If $\sigma_{x,y} = \frac{1}{4}$, then $N_{x,y}$ are very large compared to $1/\mu$ which means that the difference scheme (2) can be analyzed using standard techniques. We therefore assume that

$$\sigma_x = \upsilon_1 \mu \ln N_x, \quad \sigma_y = \upsilon_2 \mu \ln N_y.$$

Consider the mesh generating function d in the form

$$d(\xi) = 4\xi.$$

In this case the meshes $\overline{\omega}^{hx}$ and $\overline{\omega}^{hy}$ are piecewise uniform with the step sizes

$$N_x^{-1} < h_x < 2N_x^{-1}, \quad h_{x\mu} = 4\upsilon_1 \mu N_x^{-1} \ln N_x, \tag{13}$$
$$N_y^{-1} < h_y < 2N_y^{-1}, \quad h_{y\mu} = 4\upsilon_2 \mu N_y^{-1} \ln N_y.$$

Now, using (11) and (12), we estimate the truncation error $T(t)$ in (8) on the piecewise uniform mesh (13). In (13), we choose $\upsilon_{1,2} = 1/\kappa_{1,2}$. To evaluate the right-hand side in (11) on $(0, \frac{1}{2}]$, we consider the following three cases: $x_i \in (0, \sigma_x)$, $x_i = \sigma_x$ and $x_i \in (\sigma_x, \frac{1}{2}]$. If $x_i \in (0, \sigma_x)$, then $h_{x,i-1} = h_{xi} = h_{x\mu}$, and by the Taylor expansions we have

$$|I^{(x)}(x_i, y_j, t, u)| \leqslant C h_{x\mu}(1 + \mu^{-1}), \quad x_i \in (0, \sigma_x).$$

If $x_i = \sigma_x$, then $h_{x,i-1} = h_{x\mu}$, $h_{xi} = h_x$, and by the Taylor expansion and taking into account that $\sigma_x = \mu \ln N_x/\kappa_1$, we have

$$|I^{(x)}(\sigma_x, y_j, t, u)| \leqslant \frac{C}{h_{x\mu} + h_x} \left(h_{x\mu}^2 + h_x^2 + \frac{h_{x\mu}}{\mu} + \frac{h_x}{\kappa_1 N_x} \right)$$
$$\leqslant C[h_{x\mu}(1 + \mu^{-1}) + h_x + (\kappa_1 N_x)^{-1}].$$

If $x_i \in (\sigma_x, \frac{1}{2}]$, then $h_{x,i-1} = h_{xi} = h_x$, and we have

$$|I^{(x)}(x_i, y_j, t, u)| \leqslant C[h_x + (\kappa_1 N_x)^{-1}], \quad x_i \in (\sigma_x, \tfrac{1}{2}].$$

Similarly, we can prove these three estimates on the interval $[\frac{1}{2}, 1)$, and we conclude the estimate

$$|I^{(x)}(x_i, y_j, t, u)| \leqslant C[h_{x\mu}(1 + \mu^{-1}) + h_x + (\kappa_1 N_x)^{-1}], \quad x_i \in (0, 1).$$

In a similar way, using (12), we can prove the estimate

$$|I^{(y)}(x_i, y_j, t, u)| \leqslant C[h_{y\mu}(1 + \mu^{-1}) + h_y + (\kappa_2 N_y)^{-1}], \quad y_j \in (0, 1).$$

From here and (13), it follows that

$$|I^{(x)}(x_i, y_j, t, u)| \leqslant C(N_x^{-1} \ln N_x), \quad |I^{(y)}(x_i, y_j, t, u)| \leqslant C(N_y^{-1} \ln N_y),$$

and, hence, the second term in the estimate of the truncation error T in (8) on the piecewise uniform mesh (13) is estimated by

$$\tfrac{1}{2}[\|I(t)\|_{\omega^h} + \|I(t-\tau)\|_{\omega^h}] \leqslant C(N^{-1} \ln N), \quad N = \min\{N_x; N_y\}.$$

Using (10), the first term in (8) is estimated by

$$\frac{1}{6}\max_{(P,t)\in Q}|u_{ttt}(P,t)|\tau^2\leqslant C\tau^2.$$

Thus,

$$\|T(t)\|_{\omega^h}\leqslant C(N^{-1}\ln N+\tau^2),\qquad N=\min\{N_x;N_y\}. \tag{14}$$

Similarly, for $T(t)$ from (9), we can prove the estimate

$$\|T(t)\|_{\omega^h}\leqslant C(N^{-1}\ln N+\tau). \tag{15}$$

Now, we prove the theorem.

Theorem 1. *Let the time mesh spacing τ satisfy the CFL condition* (4). *Then the difference scheme* (2) *on the piecewise uniform mesh* (13) *converges μ-uniformly to the solution of* (1):

$$\max_{t\in\overline{\omega}^\tau}\|U(t)-u(t)\|_{\overline{\omega}^h}\leqslant C(N^{-1}\ln N+|\theta-0.5|\tau+\tau^2), \tag{16}$$

where $N=\min\{N_x;N_y\}$ and constant C is independent of μ, N and τ.

Proof. Introduce the notation

$$W(P,t)=U(P,t)-u(P,t).$$

Using the mean-value theorem, from (2) we conclude that $W(P,t)$ satisfies

$$\begin{aligned}(\theta\mathscr{L}^h_f(P,t)+\tau^{-1})W(P,t)=&-[(1-\theta)\mathscr{L}^h_f(P,t-\tau)-\tau^{-1}]W(P,t-\tau)\\&-T(P,t),\quad (P,t)\in\omega^h\times\omega^\tau,\end{aligned}$$

$$W(P,t)=0,\quad P\in\partial\omega^h,\quad \mathscr{L}^h_f(P,t)\equiv\mathscr{L}^h+f_u(P,t),$$

where T is the truncation error of the exact solution u to (1) and $f_u(P,t)\equiv f_u[P,t,u(P,t)+\eta(P,t)W(P,t)]$, $0<\eta(P,t)<1$. Represent the above difference equation in the following equivalent form:

$$\begin{aligned}(1+\theta r^k_{ij})W^k_{ij}=&\,\theta[\mathscr{M}^{h\tau}_x(W^k_{ij})+\mathscr{M}^{h\tau}_y(W^k_{ij})]+(1-\theta)[\mathscr{M}^{h\tau}_x(W^{k-1}_{ij})+\mathscr{M}^{h\tau}_y(W^{k-1}_{ij})]\\&+[1-(1-\theta)r^{k-1}_{ij}]W^{k-1}_{ij}-\tau T_{ij},\end{aligned}$$

$$r^k_{ij}=\tau\mu^2(v_i+w_j)+\tau f^k_{u,ij},\quad \mathscr{M}^{h\tau}_x(W^k_{ij})\equiv\tau\mu^2(v_{xi}W^k_{i+1,j}+v_{x,i-1}W^k_{i-1,j}),$$

$$\mathscr{M}^{h\tau}_y(W^k_{ij})\equiv\tau\mu^2(w_{yj}W^k_{i,j+1}+w_{y,j-1}W^k_{i,j-1}).$$

Under the CFL condition (4) all the coefficients on the right are nonnegative, and we conclude the estimate

$$\|W(t)\|_{\overline{\omega}^h}\leqslant\|W(t-\tau)\|_{\overline{\omega}^h}+\tau\|T(t)\|_{\overline{\omega}^h}.$$

Since $W(P,0)=0$, by induction we conclude that

$$\|W(t_k)\|\leqslant k\tau\max_{1\leqslant t\leqslant t_k}\|T(t)\|_{\overline{\omega}^h},\quad k=1,\dots,N_\tau.$$

Taking into account $N_\tau\tau=t_F$, we have

$$\max_{t\in\omega^\tau}\|W(t)\|\leqslant t_F\max_{1\leqslant t\leqslant t_F}\|T(t)\|_{\overline{\omega}^h}.$$

From here, (14) and (15), we prove the theorem.

3.3.2. Uniform convergence of the difference scheme (2) on the log-mesh

We choose the transition points σ_x, $(1-\sigma_x)$ and σ_y, $(1-\sigma_y)$ as in [1], i.e.,

$$\sigma_x = \upsilon_1 \mu \ln(1/\mu), \quad \sigma_y = \upsilon_2 \mu \ln(1/\mu), \tag{17}$$

$$d(\xi) = \frac{\ln[1-4(1-\mu)\xi]}{\ln \mu}.$$

Firstly, we estimate the truncation error $T(t)$ from (8) on the log-mesh (17), where $\upsilon_{1,2} = 1/\kappa_{1,2}$. The mesh points in (17) are chosen such that

$$h_{xi} \leqslant \begin{cases} 4/(\kappa_1 N_x), & i = 0, \dots, N_x/4 - 1, \\ 2/N_x, & i = N_x/4, \dots, 3N_x/4 - 1, \\ 4/(\kappa_1 N_x), & i = 3N_x/4, \dots, N_x - 1, \end{cases}$$

$$\exp(-\mu^{-1}\kappa_1 x_i) - \exp(-\mu^{-1}\kappa_1 x_{i+1}) \leqslant 4/N_x, \quad x_i \in [0, \tfrac{1}{2}],$$

$$\exp(-\mu^{-1}\kappa_1(1-x_{i+1})) - \exp(-\mu^{-1}\kappa_1(1-x_i)) \leqslant 4/N_x, \quad x_i \in [\tfrac{1}{2}, 1),$$

where we assume that $N_x \leqslant \mu^{-1}$. From here, we estimate (11) by

$$|I^{(x)}(x_i, y_j, t, u)| \leqslant \frac{C}{\kappa_1 N_x}[\max\{4(1+\kappa_1); 12\}], \quad x_i \in (0, 1).$$

In a similar way, we estimate (12) by

$$|I^{(y)}(x_i, y_j, t, u)| \leqslant \frac{C}{\kappa_2 N_y}[\max\{4(1+\kappa_2); 12\}], \quad y_j \in (0, 1).$$

From here, it follows that

$$|I^{(x)}(x_i, y_j, t, u)| \leqslant C N_x^{-1}, \quad |I^{(y)}(x_i, y_j, t, u)| \leqslant C N_y^{-1},$$

and, hence, the second term in the estimate on the truncation error T from (8) on the log-mesh (17) is estimated by

$$\tfrac{1}{2}[\|I(t)\|_{\omega^h} + \|I(t-\tau)\|_{\omega^h}] \leqslant C N^{-1}, \quad N = \min\{N_x; N_y\}.$$

Using (10), the first term in (8) is estimated by

$$\tfrac{1}{6} \max_{(P,t)\in Q} |u_{ttt}(P,t)|\tau^2 \leqslant C\tau^2.$$

Thus,

$$\|T(t)\|_{\omega^h} \leqslant C(N^{-1} + \tau^2).$$

Similarly, for $T(t)$ from (9), we can prove the estimate

$$\|T(t)\|_{\omega^h} \leqslant C(N^{-1} + \tau).$$

For the difference (2) on the log-mesh (17), Theorem 1 on μ-uniform convergence holds true with the following error estimate:

$$\max_{t \in \overline{\omega}^\tau} \|U(t) - u(t)\|_{\overline{\omega}^h} \leqslant C(N^{-1} + |\theta - 0.5|\tau + \tau^2), \quad N = \min\{N_x; N_y\}, \tag{18}$$

where constant C is independent of μ, N and τ.

4. Numerical experiments

In this section, we consider the model problem

$$-\mu^2(u_{xx}+u_{yy})+u_t=-\frac{u-4}{5-u},$$

$$(x,y,t)\in\omega\times(0,10],\quad \omega=\{0<x<1\}\times\{0<y<1\},$$

$$u(\omega,0)=0,\quad u(\partial\omega,0)=1,\quad u(\partial\omega,t)=1,\quad t\in(0,10].$$

The steady state solution to the reduced problem ($\mu=0$) is $u_r=4$. For $\mu\ll 1$ the problem is singularly perturbed and the steady state solution increases sharply from $u=1$ on $\partial\omega$ to $u=4$ on the interior. The solution to the parabolic problem approaches this steady state with time.

For the model problem, we solve the nonlinear difference (2) with the monotone iterative method, based on the method of upper and lower solutions, from [2]. The paper [2] introduced a monotone iterative method for solving the weighted average scheme. The method's parameter-uniform convergence was proved for nonlinear, two-dimensional problems. This method is a practical and robust alternative to Newton's method for solving the nonlinear algebraic system arising from the weighted average scheme at each time level.

The numerical solution at $t=t_0$ is simply given by the initial condition $V(\omega^h,t_0)=0$, $V(\partial\omega^h,t_0)=1$. The mesh function $\underline{V}^{(0)}(P,t_1)$ defined by $\underline{V}^{(0)}(P,t_1)=V(P,t_0)$, $P\in\overline{\omega}^h$, is clearly a lower solution with respect to $V(P,t_0)$. We initiate the algorithm with $\underline{V}^{(0)}(P,t_1)$ and thus generate a sequence of lower solutions. At each time level t_k, we define a converged solution $V(P,t_k)=\underline{V}^{(n_*)}(P,t_k)$ with $n_*=n_*(t_k)$ minimal subject to $\|\underline{V}^{(n_*)}(t_k)-\underline{V}^{(n_*-1)}(t_k)\|_{\overline{\omega}^h}<\delta$, where δ is a specified tolerance. At the next time level, t_{k+1}, we require an initial iterate that is a lower solution with respect to $V(P,t_k)$. Since the boundary condition and function $f(u)=(u-4)/(5-u)$ are independent of time, we may choose $\underline{V}^{(0)}(P,t_{k+1})=V(P,t_k)$, $P\in\overline{\omega}^h$. Now, from [2, Theorem 1], it follows by induction on k that the mesh function $\overline{V}(P,t_{k+1})$ defined by $\overline{V}(\omega^h,t_{k+1})=4$, $\overline{V}(\partial\omega^h,t_{k+1})=1$ is an upper solution with respect to $V(P,t_k)$ and thus our computed mesh functions satisfy

$$0\leqslant\underline{V}^{(n)}(P,t_k)\leqslant 4,\quad P\in\overline{\omega}^h,\quad 0\leqslant n\leqslant n_*,\quad 0\leqslant k\leqslant N_\tau.$$

Hence we may suppose that $f_u=1/(5-u)^2$ is bounded below and above by $c_*=\frac{1}{25}$ and $c^*=1$, respectively. Thus, the CFL condition (4) for the model problem is defined by $c^*=1$.

We take as our convergence tolerance $\delta=10^{-5}$. With either the piecewise uniform mesh (13) or log-mesh (17), we take $N_x=N_y=N$. Because of mesh nonuniformity, the linear systems may be nonsymmetric. Therefore, we solve all linear systems with the restarted GMRES(m) algorithm from [11].

4.1. Spatial order of accuracy

For each of the implicit and Crank–Nicolson schemes, we investigate the numerical order of convergence with respect to N^{-1}. Let V^N be the numerical solution computed on a mesh with $N_x=N_y=N$. We measure the error in V^N by comparing it to the reference solution V^{2N}, computed on the mesh with $N_x=N_y=2N$. With the norm

$$\|V\|=\max_{(P,t)\in\overline{\omega}^h\times\overline{\omega}^\tau}|V(P,t)|,$$

we suppose that the error $E_N\equiv\|V^N-V^{2N}\|$ satisfies

$$E_N=C(N^{-1})^p,$$

where constant C is independent of N, and p is the numerical order of convergence. For each N, we compute p_N from

$$p_N=\frac{\ln(E_N/E_{2N})}{\ln 2},$$

and we compute a μ-uniform order of convergence $\overline{p}$ as in [4]

$$\overline{p}_N = \frac{\ln(\overline{E}_N/\overline{E}_{2N})}{\ln 2},$$

where $\overline{E}_N = \max_\mu E_N$.

4.1.1. Spatial accuracy on the piecewise uniform mesh (13)

The implicit and Crank–Nicolson schemes, respectively, correspond to $\theta = 1$ and $\theta = \frac{1}{2}$ in the generic (2). We solve each of these schemes with the monotone iterative method from [2]. For each of $\mu = 10^{-2}$, 10^{-3}, 10^{-4} and 10^{-5}, we compute a sequence of solutions $\{V^N\}$, where $N = 32$, 64, 128, 256 and 512. For the boundary layer thickness, we take

$$\upsilon_1 = \upsilon_2 = \frac{9}{\sqrt{c_*}\log_2 N}$$

in (13). Thus, we choose the computational boundary layer thickness independently of N and the solution V^N may be directly compared with V^{2N}.

For the various values of μ and N, we give in Table 1 the right-hand side of the CFL condition (4). Clearly, the implicit scheme satisfies the CFL condition for all choices of time step τ. To ensure that the Crank–Nicolson scheme satisfies the CFL condition, we choose $\tau = 10^{-2}$ for all μ and N.

The error for each scheme is shown in Table 2. For $\mu \leqslant 10^{-3}$, the error is independent of μ and decreases with N. The numerical order of convergence p_N and $\overline{p}_N$ is shown in Table 3. Each scheme's numerical order of spatial accuracy is between one and two.

Table 1
The right-hand side of the CFL condition (4) for the piecewise uniform mesh (13)

$\mu\backslash N$	32	64	128	256	512
10^{-2}	7.09×10^{-1}	3.79×10^{-1}	1.32×10^{-1}	3.67×10^{-2}	9.45×10^{-3}
10^{-3}	7.92×10^{-1}	4.87×10^{-1}	1.92×10^{-1}	5.61×10^{-2}	1.46×10^{-2}
10^{-4}	7.92×10^{-1}	4.87×10^{-1}	1.92×10^{-1}	5.61×10^{-2}	1.46×10^{-2}
10^{-5}	7.92×10^{-1}	4.87×10^{-1}	1.92×10^{-1}	5.61×10^{-2}	1.46×10^{-2}

Table 2
The error E_N for the implicit and Crank–Nicolson schemes on the piecewise uniform mesh (13)

$\mu\backslash N$	32	64	128	256
Implicit scheme				
10^{-2}	1.259×10^{-1}	4.279×10^{-2}	1.237×10^{-2}	3.376×10^{-3}
10^{-3}	1.467×10^{-1}	6.346×10^{-2}	1.843×10^{-2}	5.128×10^{-3}
10^{-4}	1.467×10^{-1}	6.346×10^{-2}	1.843×10^{-2}	5.128×10^{-3}
10^{-5}	1.467×10^{-1}	6.346×10^{-2}	1.843×10^{-2}	5.128×10^{-3}
Crank–Nicolson scheme				
10^{-2}	1.260×10^{-1}	4.287×10^{-2}	1.240×10^{-2}	3.388×10^{-3}
10^{-3}	1.469×10^{-1}	6.353×10^{-2}	1.847×10^{-2}	5.127×10^{-3}
10^{-4}	1.469×10^{-1}	6.353×10^{-2}	1.847×10^{-2}	5.127×10^{-3}
10^{-5}	1.469×10^{-1}	6.353×10^{-2}	1.847×10^{-2}	5.127×10^{-3}

The time step is $\tau = 10^{-2}$.

Table 3
The numerical order of convergence p_N and $\overline{p}_N$ for the implicit and Crank–Nicolson schemes on the piecewise uniform mesh (13)

$\mu\backslash N$	Implicit scheme			Crank–Nicolson scheme		
	32	64	128	32	64	128
10^{-2}	1.556	1.791	1.873	1.555	1.790	1.872
10^{-3}	1.209	1.784	1.846	1.209	1.783	1.849
10^{-4}	1.209	1.784	1.846	1.209	1.783	1.849
10^{-5}	1.209	1.784	1.846	1.209	1.783	1.849
$\overline{p}_N$	1.209	1.784	1.815	1.209	1.783	1.849

The time step is $\tau = 10^{-2}$.

Table 4
The right-hand side of the CFL condition (4) for the log-mesh (17)

$\mu\backslash N$	32	64	128	256	512
10^{-2}	1.12×10^{-1}	2.65×10^{-2}	6.33×10^{-3}	1.54×10^{-3}	3.80×10^{-4}
10^{-3}	1.14×10^{-1}	2.70×10^{-2}	6.45×10^{-3}	1.57×10^{-3}	3.87×10^{-4}
10^{-4}	1.14×10^{-1}	2.71×10^{-2}	6.46×10^{-3}	1.57×10^{-3}	3.87×10^{-4}
10^{-5}	1.14×10^{-1}	2.71×10^{-2}	6.46×10^{-3}	1.57×10^{-3}	3.87×10^{-4}

Table 5
The error E_N for the implicit and Crank–Nicolson schemes on the log-mesh (17)

μ/N	32	64	128	256
Implicit scheme				
10^{-2}	1.012×10^{-2}	2.485×10^{-3}	6.219×10^{-4}	1.553×10^{-4}
10^{-3}	1.029×10^{-2}	2.535×10^{-3}	6.331×10^{-4}	1.581×10^{-4}
10^{-4}	1.031×10^{-2}	2.540×10^{-3}	6.342×10^{-4}	1.584×10^{-4}
10^{-5}	1.031×10^{-2}	2.541×10^{-3}	6.343×10^{-4}	1.584×10^{-4}
Crank–Nicolson scheme				
10^{-2}	1.013×10^{-2}	2.485×10^{-3}	6.219×10^{-4}	1.553×10^{-4}
10^{-3}	1.029×10^{-2}	2.535×10^{-3}	6.331×10^{-4}	1.581×10^{-4}
10^{-4}	1.031×10^{-2}	2.540×10^{-3}	6.342×10^{-4}	1.584×10^{-4}
10^{-5}	1.031×10^{-2}	2.541×10^{-3}	6.343×10^{-4}	1.584×10^{-4}

The time step is $\tau = 5 \times 10^{-4}$.

4.1.2. Spatial accuracy on the log-mesh (17)

For the boundary layer thickness, we take

$$\upsilon_1 = \upsilon_2 = \frac{1}{\sqrt{c_*}}$$

in (17). Thus, the computational boundary layer thickness is independent of N and the solution V^N may be directly compared with V^{2N}.

For the various values of μ and N, we present in Table 4 the right-hand side of the CFL condition (4). To ensure that the Crank–Nicolson scheme satisfies the CFL condition, we choose $\tau = 5 \times 10^{-4}$ for all μ and N.

The error for each scheme is shown in Table 5 and the numerical order of convergence is shown in Table 6. Each scheme's numerical order of spatial accuracy is very close to two.

Now, the results of Table 3 on the piecewise uniform mesh and Table 6 on the log-mesh are with $\tau = 10^{-2}$ and $\tau = 5 \times 10^{-4}$, respectively. To check that the numerical order of convergence is independent of τ, we repeated the

Table 6
The numerical order of convergence p_N and $\overline{p}_N$ for the implicit and Crank–Nicolson schemes on the log-mesh (17)

$\mu\backslash N$	Implicit scheme			Crank–Nicolson scheme		
	32	64	128	32	64	128
10^{-2}	2.026	1.999	2.001	2.026	1.999	2.001
10^{-3}	2.021	2.002	2.002	2.021	2.002	2.002
10^{-4}	2.021	2.002	2.001	2.021	2.002	2.001
10^{-5}	2.021	2.002	2.001	2.021	2.002	2.001
$\overline{p}_N$	2.021	2.002	2.001	2.021	2.002	2.001

The time step is $\tau = 5 \times 10^{-4}$.

Table 7
The error E_N for the implicit and Crank–Nicolson schemes on the log-mesh (17)

μ/N	32	64	128	256
Implicit scheme				
10^{-2}	1.012×10^{-2}	2.484×10^{-3}	6.215×10^{-4}	1.552×10^{-4}
10^{-3}	1.028×10^{-2}	2.533×10^{-3}	6.326×10^{-4}	1.580×10^{-4}
10^{-4}	1.030×10^{-2}	2.538×10^{-3}	6.337×10^{-4}	1.583×10^{-4}
10^{-5}	1.030×10^{-2}	2.539×10^{-3}	6.338×10^{-4}	1.583×10^{-4}
Crank–Nicolson scheme				
10^{-2}	1.012×10^{-2}	2.485×10^{-3}	6.219×10^{-4}	1.553×10^{-4}
10^{-3}	1.029×10^{-2}	2.535×10^{-3}	6.331×10^{-4}	1.581×10^{-4}
10^{-4}	1.031×10^{-2}	2.540×10^{-3}	6.342×10^{-4}	1.584×10^{-4}
10^{-5}	1.031×10^{-2}	2.541×10^{-3}	6.343×10^{-4}	1.584×10^{-4}

The time step is $\tau = 10^{-2}$.

log-mesh experiments with $\tau = 10^{-2}$. The error and numerical order of convergence are shown in Tables 7 and 8, respectively. The values are very similar to those of Tables 5 and 6. We thus conclude that the spatial accuracy is independent of τ. This also demonstrates that the CFL condition (4) is not strictly necessary for stability.

4.2. Order of accuracy with respect to τ

We consider now the temporal accuracy of the implicit and Crank–Nicolson schemes on the piecewise uniform mesh. In the absence of an exact solution for the model problem, the Crank–Nicolson scheme with $\tau_* = 10^{-3}$ is solved with the monotone iterative method from [2] for 5000 time steps. This generates a reference solution $V_{\tau_*}(P, t)$ for $0 \leqslant t \leqslant 5$. With $n_* = 4$ iterations on each time step, the reference solution is fully converged. We then generate "coarse" solutions $V_\tau(P, t)$ by taking $\tau_1 = 0.1$ or $\tau_2 = 0.04$ and solving both the implicit scheme and the Crank–Nicolson scheme with the corresponding monotone iterative method. At the common times, $t = 0.2, 0.4, \ldots, 5.0$, each of these solutions is compared with $V_{\tau_*}(P, t)$.

In Tables 9 and 10, for the implicit scheme with $N = 256$ and 512, we present the maximum error $E_\tau(t) = \| V_\tau(t) - V_{\tau_*}(t)\|_{\overline{\omega}^h}$, $\tau = \tau_1$ and $\tau = \tau_2$, as a function of t. As t increases, the ratio E_{τ_1}/E_{τ_2} tends to $\tau_1/\tau_2 = 2.5$, consistent with first order convergence with respect to τ.

In Tables 11 and 12, for the Crank–Nicolson scheme with $N = 256$ and 512, we present the maximum error $E_\tau(t) = \| V_\tau(t) - V_{\tau_*}(t)\|_{\overline{\omega}^h}$, $\tau = \tau_1$ and $\tau = \tau_2$ as a function of t. As t increases, the ratio E_{τ_1}/E_{τ_2} tends to $(\tau_1/\tau_2)^2 = 6.25$, consistent with second order convergence with respect to τ.

In Fig. 1 we plot E_τ against t for each of the schemes and time steps τ. This demonstrates the improved accuracy of the Crank–Nicolson scheme with respect to the implicit scheme.

Table 8
The numerical order of convergence p_N and $\overline{p}_N$ for the implicit and Crank–Nicolson schemes on the log-mesh (17)

$\mu\backslash N$	Implicit scheme			Crank–Nicolson scheme		
	32	64	128	32	64	128
10^{-2}	2.026	1.999	2.001	2.026	1.999	2.002
10^{-3}	2.021	2.002	2.002	2.021	2.002	2.002
10^{-4}	2.021	2.002	2.001	2.021	2.002	2.002
10^{-5}	2.021	2.002	2.001	2.021	2.002	2.002
$\overline{p}_N$	2.021	2.002	2.001	2.021	2.002	2.002

The time step is $\tau = 10^{-2}$.

Table 9
The error $E_\tau(t)$ for the implicit scheme with $N = 256$

t	E_{τ_1}	E_{τ_2}	E_{τ_1}	E_{τ_2}	E_{τ_1}/E_{τ_2}
0.2	8.799×10^{-2}	3.695×10^{-2}	8.948×10^{-2}	3.746×10^{-2}	2.39
0.4	6.018×10^{-2}	2.517×10^{-2}	5.792×10^{-2}	2.472×10^{-2}	2.34
0.6	4.414×10^{-2}	1.859×10^{-2}	4.389×10^{-2}	1.797×10^{-2}	2.44
0.8	3.837×10^{-2}	1.565×10^{-2}	3.785×10^{-2}	1.563×10^{-2}	2.42
1.0	3.297×10^{-2}	1.358×10^{-2}	3.327×10^{-2}	1.349×10^{-2}	2.47
2.0	2.413×10^{-2}	9.771×10^{-3}	2.429×10^{-2}	9.809×10^{-3}	2.48
3.0	2.141×10^{-2}	8.613×10^{-3}	2.140×10^{-2}	8.617×10^{-3}	2.48
4.0	2.027×10^{-2}	8.137×10^{-3}	2.023×10^{-2}	8.119×10^{-3}	2.49
5.0	1.924×10^{-2}	7.720×10^{-3}	1.924×10^{-2}	7.718×10^{-3}	2.49
μ	10^{-2}		$\leqslant 10^{-3}$		

Table 10
The error $E_\tau(t)$ for the implicit scheme with $N = 512$

t	E_{τ_1}	E_{τ_2}	E_{τ_1}	E_{τ_2}	E_{τ_1}/E_{τ_2}
0.2	1.017×10^{-1}	4.599×10^{-2}	1.033×10^{-1}	4.419×10^{-2}	2.34
0.4	6.336×10^{-2}	2.625×10^{-2}	6.213×10^{-2}	2.565×10^{-2}	2.42
0.6	4.730×10^{-2}	1.940×10^{-2}	4.705×10^{-2}	1.920×10^{-2}	2.45
0.8	3.914×10^{-2}	1.598×10^{-2}	3.916×10^{-2}	1.600×10^{-2}	2.45
1.0	3.425×10^{-2}	1.391×10^{-2}	3.415×10^{-2}	1.396×10^{-2}	2.45
2.0	2.449×10^{-2}	9.883×10^{-3}	2.449×10^{-2}	9.888×10^{-3}	2.48
3.0	2.160×10^{-2}	8.693×10^{-3}	2.159×10^{-2}	8.687×10^{-3}	2.49
4.0	2.033×10^{-2}	8.161×10^{-3}	2.033×10^{-2}	8.162×10^{-3}	2.49
5.0	1.928×10^{-2}	7.734×10^{-3}	1.928×10^{-2}	7.734×10^{-3}	2.49
μ	10^{-2}		$\leqslant 10^{-3}$		

5. Conclusions

From the numerical evidence, we make the following observations:

- Although the theoretical estimate (16) predicts almost first order spatial accuracy of the implicit and Crank–Nicolson schemes on the piecewise uniform mesh (13), the numerical experiments indicate that the spatial accuracy is between one and two.

Table 11
The error $E_\tau(t)$ for the Crank–Nicolson scheme with $N = 256$

t	E_{τ_1}	E_{τ_2}	E_{τ_1}	E_{τ_2}	E_{τ_1}/E_{τ_2}
0.2	1.833×10^{-2}	2.728×10^{-3}	1.477×10^{-2}	2.724×10^{-3}	5.42
0.4	5.097×10^{-3}	8.320×10^{-4}	4.609×10^{-3}	7.208×10^{-4}	6.39
0.6	2.486×10^{-3}	4.065×10^{-4}	2.569×10^{-3}	4.121×10^{-4}	6.23
0.8	1.503×10^{-3}	2.397×10^{-4}	1.465×10^{-3}	2.357×10^{-4}	6.22
1.0	1.061×10^{-3}	1.696×10^{-4}	1.021×10^{-3}	1.630×10^{-4}	6.26
2.0	3.237×10^{-4}	5.201×10^{-5}	3.277×10^{-4}	5.252×10^{-5}	6.24
3.0	1.654×10^{-4}	2.726×10^{-5}	1.664×10^{-4}	2.701×10^{-5}	6.16
4.0	9.977×10^{-5}	1.641×10^{-5}	9.903×10^{-5}	1.654×10^{-5}	5.99
5.0	7.694×10^{-5}	1.785×10^{-5}	7.677×10^{-5}	1.183×10^{-5}	6.49
μ	10^{-2}		$\leqslant 10^{-3}$		

Table 12
The error $E_\tau(t)$ for the Crank–Nicolson scheme with $N = 512$

t	E_{τ_1}	E_{τ_2}	E_{τ_1}	E_{τ_2}	E_{τ_1}/E_{τ_2}
0.2	1.901×10^{-1}	3.504×10^{-3}	9.318×10^{-2}	3.378×10^{-3}	27.58
0.4	7.023×10^{-2}	9.006×10^{-4}	2.380×10^{-2}	9.032×10^{-4}	26.35
0.6	2.929×10^{-2}	4.238×10^{-4}	7.069×10^{-3}	4.210×10^{-4}	16.79
0.8	1.318×10^{-2}	2.536×10^{-4}	2.304×10^{-3}	2.532×10^{-4}	9.10
1.0	6.254×10^{-3}	1.730×10^{-4}	1.066×10^{-3}	1.723×10^{-4}	6.19
2.0	3.305×10^{-4}	5.339×10^{-5}	3.305×10^{-4}	5.308×10^{-5}	6.23
3.0	1.668×10^{-4}	2.713×10^{-5}	1.667×10^{-4}	2.705×10^{-5}	6.16
4.0	1.001×10^{-4}	1.552×10^{-5}	9.986×10^{-5}	1.669×10^{-5}	5.98
5.0	7.727×10^{-5}	1.188×10^{-5}	7.717×10^{-5}	1.191×10^{-5}	6.48
μ	10^{-2}		$\leqslant 10^{-3}$		

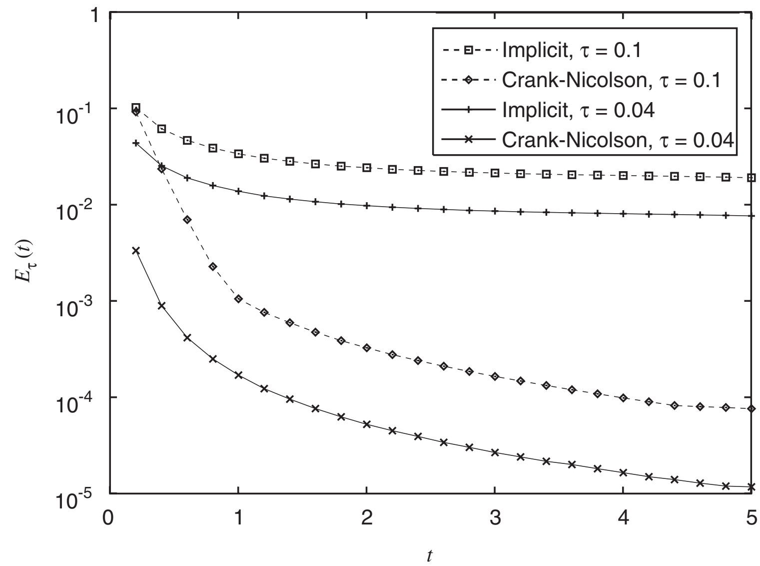

Fig. 1. The value of $E_\tau(t) = \|V_\tau(t) - V_{\tau_*}(t)\|_{\overline{\omega}^h}$ as a function of t for each of the schemes with $\tau = 0.1$ and $\tau = 0.04$.

- Similarly, although the estimate (18) predicts first order spatial accuracy of the implicit and Crank–Nicolson schemes on the log-mesh (17), the numerical experiments indicate a spatial accuracy of two.
- On the piecewise uniform mesh (13), the numerical experiments confirm that the implicit scheme is first order convergent with respect to the time step τ while the Crank–Nicolson scheme is second order convergent with respect to τ.
- For the Crank–Nicolson scheme, the time step τ can exceed the CFL condition (4) by an order of magnitude without loss of stability. (For the implicit scheme, of course, the CFL condition imposes no restriction on τ.)

References

[1] I.P. Boglaev, Finite difference domain decomposition algorithms for a parabolic problem with boundary layers, Comput. Math. Appl. 36 (1998) 25–40.
[2] I.P. Boglaev, A monotone weighted average method for a non-linear reaction–diffusion problem, Int. J. Comput. Math. 82 (2005) 1017–1031.
[3] J. Crank, P. Nicolson, A practical method for numerical evaluation of solutions of partial differential equations of the heat-conduction type, Proc. Camb. Philos. Soc. 43 (1947) 50–67.
[4] P.A. Farrell, A.F. Hegarty, J.J.H. Miller, E. O'Riordan, G.I. Shishkin, Robust Computational Techniques for Boundary Layers, CRC Press, Boca Raton, FL, 2000.
[5] N.V. Kopteva, On the uniform in small parameter convergence of a weighted scheme for the one-dimensional time-dependent convection-diffusion equation, Comput. Math. Math. Phy. 37 (1997) 1173–1180.
[6] O.A. Ladyženskaja, V.A. Solonnikov, N.N. Ural'ceva, Linear and Quasi-Linear Equations of Parabolic Type, Academic Press, New York, 1968.
[7] J.J.H. Miller, E. O'Riordan, G.I. Shishkin, Fitted Numerical Methods for Singular Perturbation Problems, World Scientific, Singapore, 1996.
[8] K.W. Morton, D.F. Mayers, Numerical Solution of Partial Differential Equations, Cambridge University Press, New York, 1995.
[9] H.-G. Roos, M. Stynes, L. Tobiska, Numerical Methods for Singularly Perturbed Differential Equations, Springer, Heidelberg, 1996.
[10] H.-G. Roos, T. Linss, Sufficient conditions for uniform convergence on layer adapted grids, Computing 64 (1999) 27–45.
[11] Y. Saad, M.H. Schultz, GMRES: a generalized minimal residual method for solving nonsymmetric linear systems, SIAM J. Sci .Statist. Comput. 7 (1986) 856–869.
[12] G.I. Shishkin, Grid approximations of singularly perturbed elliptic and parabolic equations, Russian Academy of Sciences (Ural Branch), Ekaterinburg, 1992 (in Russian).